

Supplementary Information

¹⁵N NMR relaxation results

As shown in Supplementary Figures S2 and Supplementary Tables S1-S2, the N- and C-terminal residues (i.e. residues 1-6 and 70-73, respectively) experience rapid internal fluctuations on the ps-ns time scale, as assessed by characteristically low heteronuclear ¹⁵N-[¹H]-nOe and spectral density function $J_{\text{eff}}(0)$, and $J(0.87\omega_{\text{H}}) > 6$ ps/rad. The rapid and large amplitude internal motions observed for N- and C-terminal backbone amides are consistent with the lack of observable long-range ¹H-¹H-nOes and near random coil chemical shifts observed for these residues, i.e. NMR features that are characteristic of disordered random-coil-like polypeptide segments.

The other backbone amides (residues 16-69) display relatively uniform relaxation profiles that are typical for well-folded segments of a protein with limited internal flexibility, except for a few subtle but potentially important differences for certain residues. The ¹⁵N NMR relaxation parameters measured for the amides in helices $\alpha 2$ and $\alpha 3$ yield rather uniform general order parameters (S^2) approaching 1, indicating that ps-ns internal motions of backbone atoms in these two helices are highly restricted. Interestingly, several backbone amides within the $\alpha 1$ helix and the $\alpha 1$ - $\alpha 2$ turn deviate slightly from this trend. In particular, residues 21, 25, 26, 29, 32, 33 and 34 display lower $J(0.87\omega_{\text{H}})$ (≤ 4 ps/rad) and higher $J_{\text{eff}}(0)$ (> 5.6 ns/rad), indicating that amides in this region may be experiencing slower μ s-ms motions typical of chemical exchange (Figure S2). In agreement with these results, ModelFree fitting of the ¹⁵N NMR relaxation data indicates that several of the same residues are best fit by invoking an R_{ex} term (1) (see Supplementary Table S3). Lastly, backbone amides within the N-terminal β -sheet region (residues 10-16) display elevated $J(0.87\omega_{\text{H}})$ and low $J_{\text{eff}}(0)$ (Fig. 10). This is similar, although not to the same extent, to

what is observed for amides in the N- and C-termini of the protein, suggesting that this region is relatively more flexible than the core of the protein and experiencing greater ps-ns NH bond vector internal motions than core amides. It is tempting to speculate that the enhanced flexibility of the DNA binding domain of E73 spanning the anti-parallel β -sheet region of the protein may be important for specific recognition and binding of E73's cognate DNA target.

Although ModelFree fitting of these residues yields high S^2 values (i.e. restricted flexibility), several of these NH backbone amides are best fit with higher order models (models 3-5), indicating the presence of more complex motions that are not parametrized adequately by the ModelFree formalism, and therefore put into question the reliability and significance of high S^2 for these residues (1).

These data are consistent with the backbone dynamics and thermostability data reported in the literature for several other RHH proteins. For example, an extensive structural and stability investigation of ORF56, a small RHH protein from the hyperthermophilic archaeon *Sulfolobus islandicus*, indicated that ORF56 possesses very similar backbone amide dynamics profiles to that of E73 and is an extremely stable protein. The GndHCl denaturation midpoint measured for ORF56 is ~5M which differs only slightly from the 4.8M denaturation midpoint of E73. In addition, the internal dynamics profile of E73, including all the measured ¹⁵NMR relaxation parameters, the derived reduced spectral density functions, and the calculated Lipari-Szabo motional parameters, are almost identical to that of SvtR, a protein found in the rod-shaped virus SIRV1, which too infects *Sulfolobus islandicus*, a archeal organism thriving in acidic hot springs at 85°C. In contrast, the structural and internal dynamics studies reported by Oberer et al. (2) on the mesophilic anti-toxin protein ParD, which contains a N-terminal RHH domain, indicate that even though ParD is comprised of a well structured RHH domain in solution, this domain is

more flexible as assessed by ^{15}N NMR relaxation measurements than that of E73, ORF56, or SvtR. An earlier study reported the thermodynamic characteristics of ParD (3) and revealed that the thermal denaturation mid-point (T_m) of ParD is 64°C (2) which is significantly less than the thermostability and T_m of ORF56 from *Sulfolobus islandicus* (4) and E73 from SSV-RH (this study). Altogether, these data indicate that it is reasonable to correlate restricted internal flexibility with the higher thermostability of crenarchaeal proteins such as E73.

References Cited in Supplementary Information Section

1. Mandel, A. M., Akke, M., and Palmer, A. G. (1995) Backbone dynamics of Escherichia coli ribonuclease HI: correlations with structure and function in an active enzyme, *J. Mol. Biol.* 246, 144-163.
2. Oberer, M., Zangger, K., Gruber, K., and Keller, W. (2007) The solution structure of ParD, the antidote of the ParDE toxin-antitoxin module, provides the structural basis for DNA and toxin binding, *Protein Sci.* 16, 1676-1688.
3. Oberer, M., Lindner, H., Glatter, O., Krafky, C., and Keller, W. (1999) Thermodynamic properties and DNA binding of the ParD protein from the broad host-range plasmid RK2/RP4 killing system, *J. Biol. Chem.* 380, 1413-1420.
4. Zeeb, M., Lipps, G., Lilie, H., and Balbach, J. (2004) Folding and association of an extremely stable dimeric protein from *Sulfolobus islandicus*, *J. Mol. Biol.* 336, 227-240.

Supplementary Tables S0-S3 consist of:

Table S0 – Parameters used in the molecular dynamics scheme (anneal.inp) and the non crystallographic symmetry (ncs.def) matrix used in the structural calculations of E73.

Table S1 - ^{15}N NMR relaxation parameters ($^{15}\text{N-T}_1$, $^{15}\text{N-T}_2$, $^{15}\text{N-}\{^1\text{H}\}$ -nOe) measured for SSV-RH E73 at pH 5.0 and $T = 312\text{K}$.

Table S2 - Reduced spectral density functions, $J_{\text{eff}}(0)$, $J(\omega_{\text{N}})$ and $J(0.87\omega_{\text{H}})$, tabulated from the ^{15}N NMR relaxation data obtained for E73 at a magnetic field strength of 14.1 T.

Table S3 - Motional parameters (S^2 , τ_e , R_{ex} , and model selection) computed for E73 and derived from ModelFree analysis of ^{15}N NMR relaxation parameters.

Supplementary Figures S1-S6 and Figure Legends

Supplementary Figure S1: Summary of amide H/D exchange data, patterns of sequential and short range NOEs, and $^{13}\text{C}\alpha/\beta$ and $^1\text{H}\alpha$ chemical shifts differences from random coil values for SSV-RH E73. The protein sequence is indicated on the top row using the one-letter amino acid code. Filled stars denote residues for which the amide proton exchange time constant is >20 min. nOe connectivities are diagrammed in the next eight rows. The height of the box reflects the intensity of the cross-peak classified as strong (tallest), medium, weak, and very weak (shortest): sequential $d_{\text{NN}}(i, i+1)$, $d_{\alpha\text{N}}(i, i+1)$, and $d_{\beta\text{N}}(i, i+1)$; short-range $d_{\text{NN}}(i, i+2)$, $d_{\alpha\text{N}}(i, i+2)$, $d_{\alpha\text{N}}(i, i+3)$, $d_{\alpha\beta}(i, i+3)$, and $d_{\alpha\text{N}}(i, i+4)$ are depicted from the first residue involved to the appropriate downstream residue. Bottom; Differences in parts per million (ppm) in $^1\text{H}\alpha$, $^{13}\text{C}\alpha$, and $^{13}\text{C}\beta$ chemical shifts relative to random coil values are shown in the rows labeled $\Delta^{13}\text{C}\alpha$, $\Delta^{13}\text{C}\beta$ and $\Delta^1\text{H}\alpha$, respectively. The thinnest line corresponds to no significant chemical shift difference; residues for which no line is given have not been assigned $^1\text{H}\alpha$, $^{13}\text{C}\alpha$, or $^{13}\text{C}\beta$ chemical shifts.

Regions of the protein identified as α -helices or extended β -strand by PROCHECK_NMR analysis are schematically depicted in the last row.

Supplementary Figure S2: Spectral density functions (J) at $0.87\omega_H$, ω_N and 0 frequencies obtained from ^{15}N relaxation data measured at a magnetic field of 14.1 T and plotted against residue number (Figure S2A, S2B, and S2C, respectively). Dotted lines represent spectral density values corresponding to \pm one standard deviation.

Supplementary Figure S3: Conformational exchange (R_{ex}) and order (S^2) Lipari-Szabo parameters for E73 plotted against residue number. Secondary structure elements are depicted above each plot (cylinders = α -helices and arrow = β -strand). Error bars indicate the uncertainties propagated from intrinsic errors in measured ^{15}N relaxation data.

Supplementary Figure S4: ^{15}N NMR relaxation parameters for E73 as a function of residue number. (A) Plot of ^{15}N - $[^1\text{H}]$ -nOes; and (B) ^{15}N T_1 - T_2 ratios. Plotted error bars correspond to errors reported in Tables S1, and calculated as described in Goel et al. (2010) *Biochemistry* 49, 5140-5153. Secondary structural elements of E73 are depicted as arrow (β -strand) and cylinders (α -helices) above each plot.

Supplementary Figure S5: Structure-based alignment of the amino acid sequence of E73 to that of several of its closest RHH analogs including ones that contain a 3rd helix. Amino acids are depicted in their one letter code; Capital letters indicate structurally conserved residues among the different RHH proteins; Small letters indicate that these residues are not conserved among

RHH homologs. It is interesting to note that many residues that make up the 3rd helix of E73 are not conserved among other RHH proteins containing a 3rd helix, providing further evidence that the 3rd helix of E73 plays a unique structural and functional role.

The structural alignment model also highlights residues in each protomer of the E73 that may form specific contacts with major groove DNA bases, including Lys11, Thr13, Ala15 (highlighted in the open boxed areas). Conserved hydrophobic residues include Leu 14 and Phe 16 (located in the turn region between the extended β -strand and the α 1 helix of each protomer of E73), Leu 24 (from α 1), and Ile 38, Val 43, and Leu 47 (from α 2) (and boxed in yellow). These residues follow the typical sequence conservation patterns identified in RHH transcription factors (reviewed in Schreiter & Drennan (2007) *Nat. Rev. Microbiol.* 5, pp. 710-720). Asterisks refer to residues that are discussed in the text regarding the superpositional docking model of E73 onto PutA DNA.

Supplementary Figure S6: (A) Ribbon representation of the three dimensional structure of E73 with sidechains of amino acids that may be involved in specific DNA interactions labeled in yellow. Particularly notable are the cluster of lysines (K9, K10, K11), and conserved residues T13, and A15 as the latter (i.e. K11, T13, A15) correspond to conserved residue positions 2, 4, 6 of the canonical sequence alignment characterizing RHH transcription factors (see Figure 1 of the Schreiter & Drennan (2007) review for details).

(B) Molecular surface representation of E73 indicating the location of the positively charged K11/K11' residues that have been mutated in the E73K11E variant to negatively charged glutamic acids, resulting in the abrogation of non-specific binding to viral DNA.

Figure S1

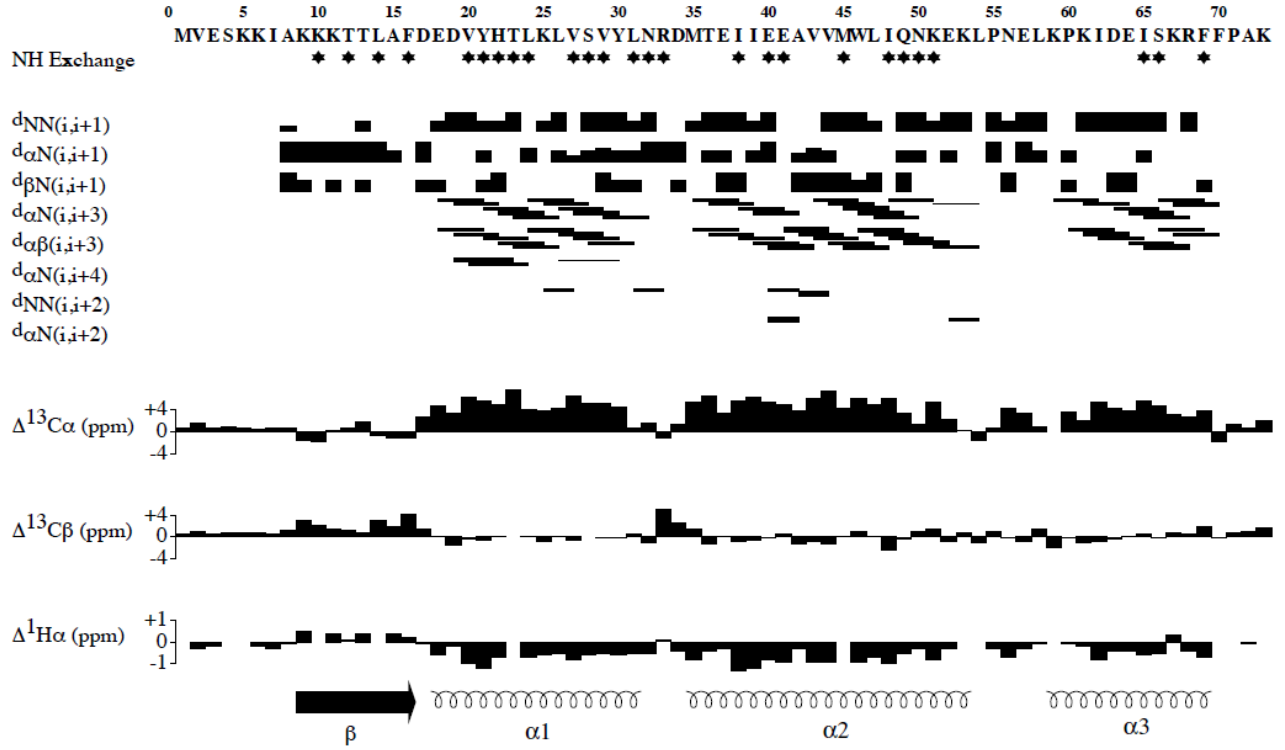


Figure S2

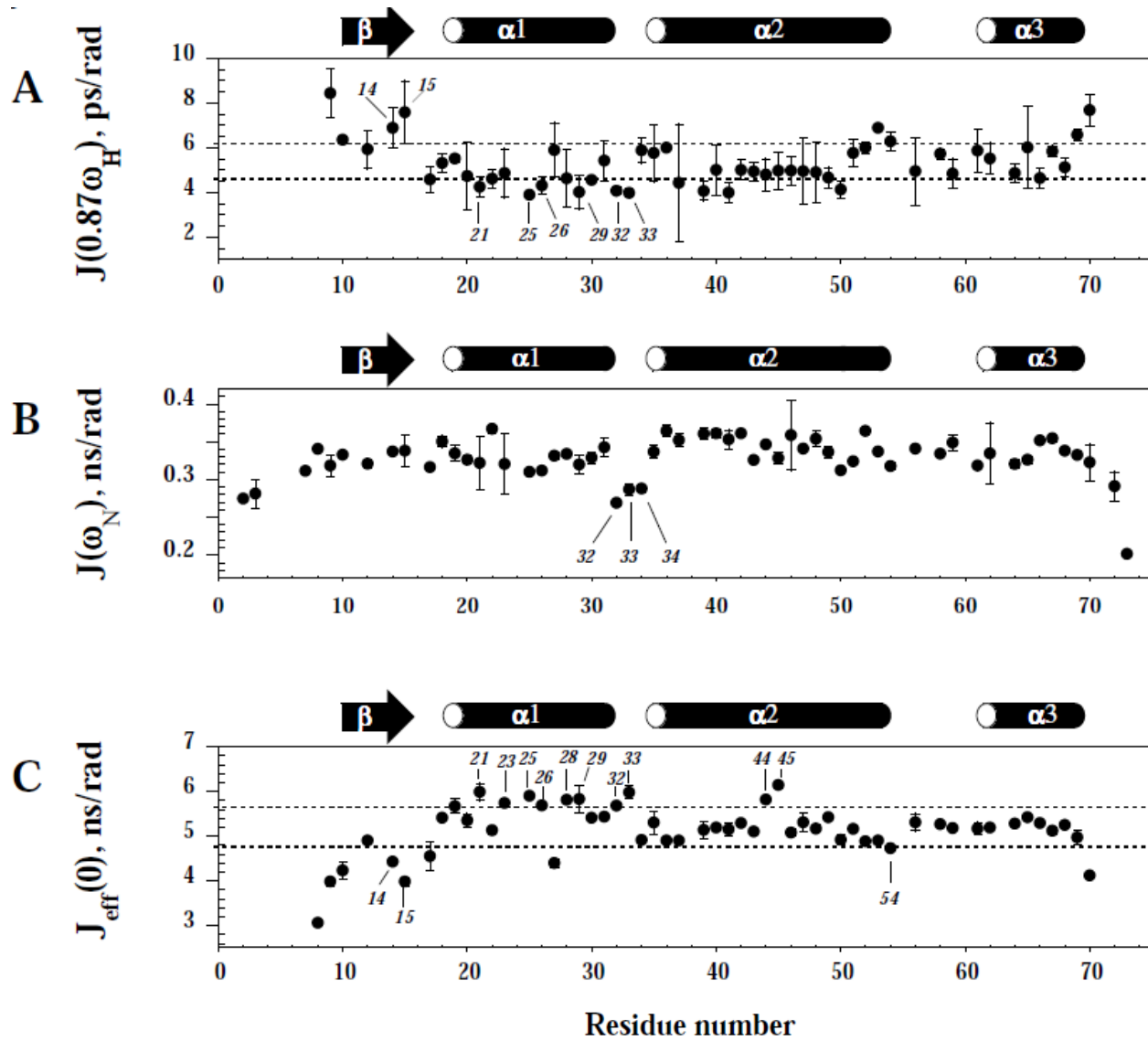
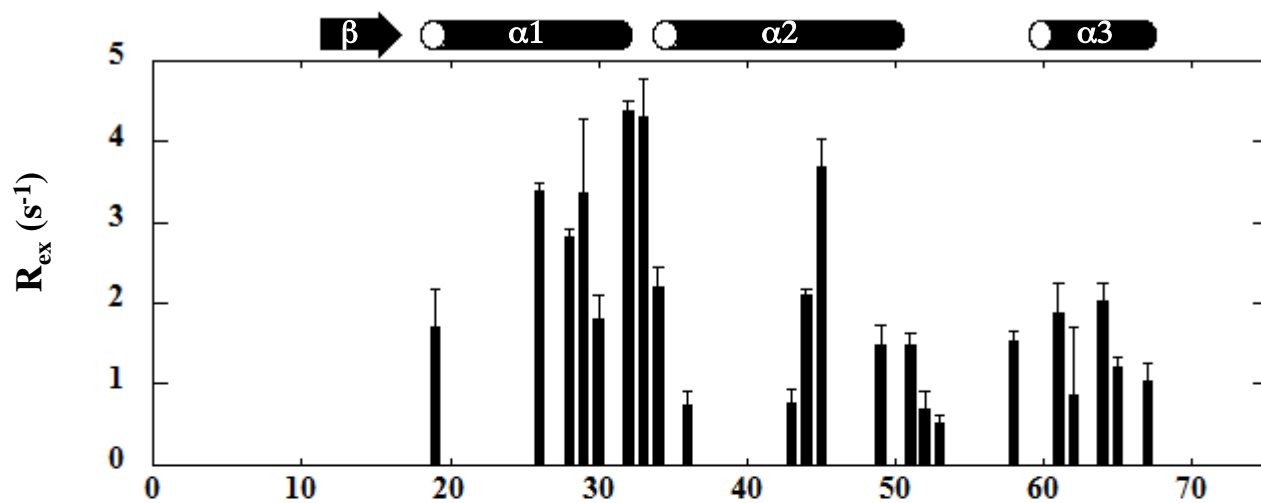


Figure S3

A



B

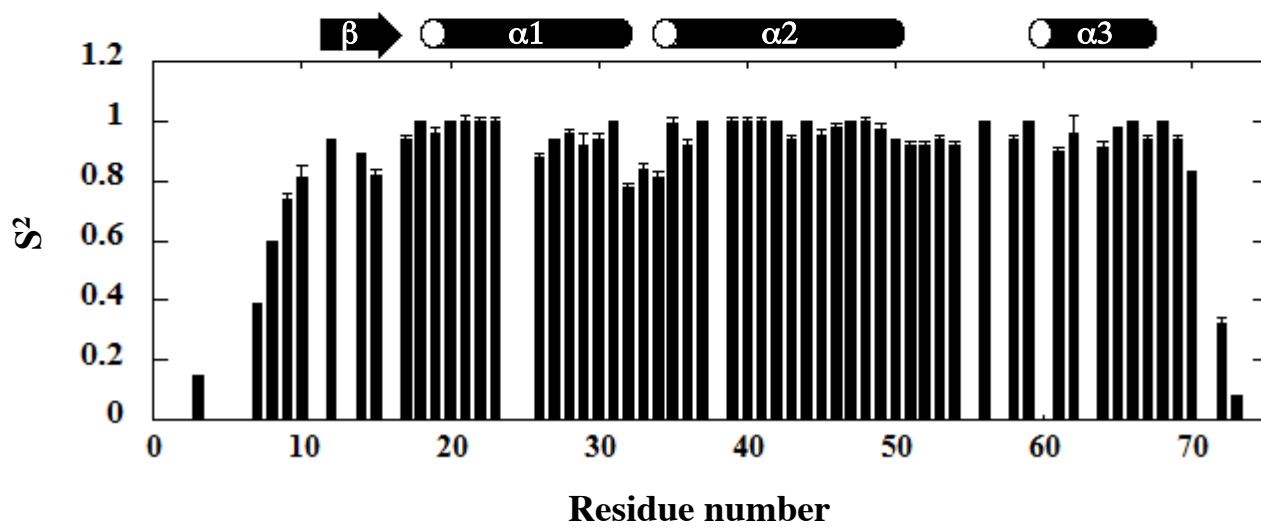
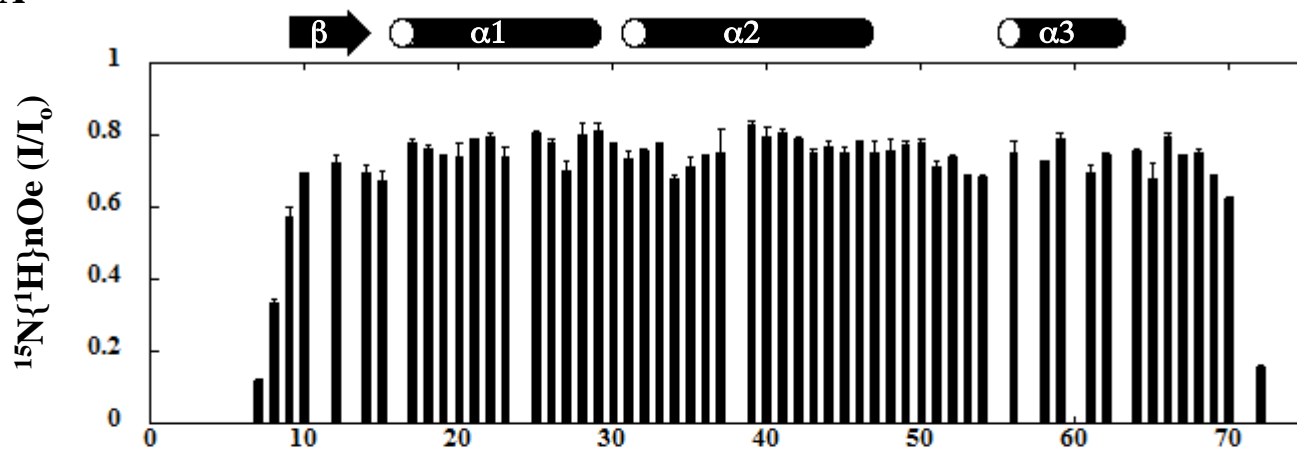


Figure S4

A



B

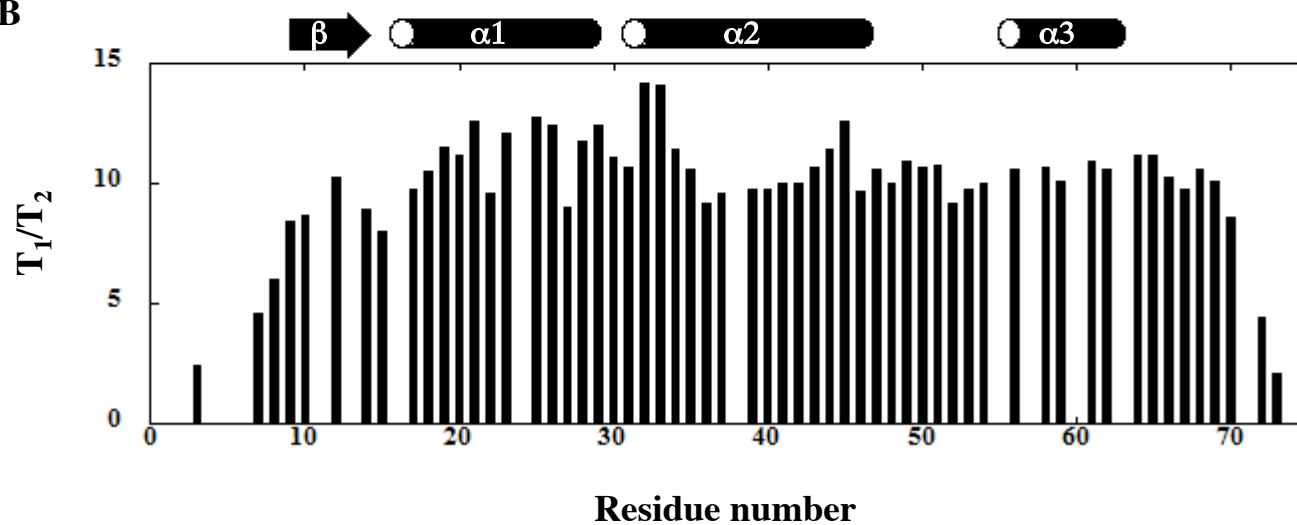


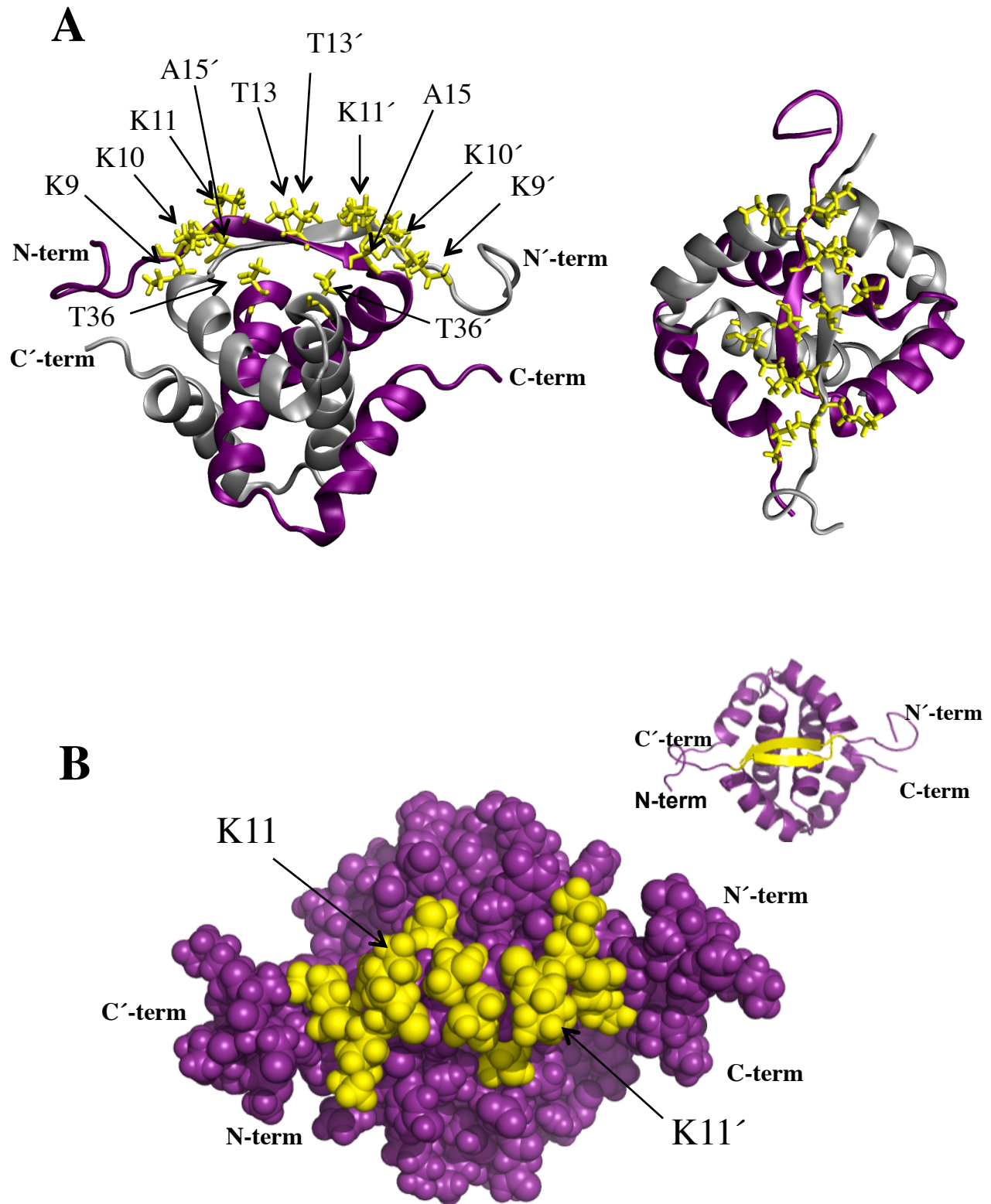
Figure S5

```

**   ***  *  *
>E73  mveskkiAKKKTTLAF DEDVYHTLKLVSFY----LN-----RDMTEIEEAVVMWLIQNK---EKL Pnelkpkideiskrffpak
>PutA  GTTTMGVKLDDATRERTKSAATR----ID-----RTPHWLIKQATFSYLEQLE---NSDT
>NikR  MORVTITLDDDLLETLDLSQR----RG-----YnNRSEAIRDILRSALAQE---ATQ
>ParD  KMPOFNLRMPREVLDLVRKVAEE----NG-----RSVNSEIYQRYMESFKKEG---R
>VirC2 eksIIVQTSRMFPVSLIEARNHFDPlgleta----rAFGHKLATAALACFARE---KATN
>SVTR  KQKAVFGIYMDKDLKTRLKVYCAK----NN-----LQLTQAIIEEATKEYLQKRN---G
>RelB  MGSINLRIDDELKARSYAALEK----MG-----VTPSEALRLMEYIADNER
>MntR  ARDDPHFNFRMPMEVREKLKFRAEA----NG-----RSMNSELLQIVQDALSKPSpvtGYRN--dAERLADEQSE--lv
>Orf56  LNGIKLGVYIPQEWHDRLMEIAKEKNLTLSD----VCRLAIKEYLDNHD
>CcdA  MKQRITVTVDSdSYQLLKAYDV.----...-----nISGLVSTTMQNEARRLR-----aERWKvenaqgmvevarfiemngsfadenkdw
>1y9b  TTLPRITARVDVDTODLAKAAAL----AG-----XsSINSFVLNAIEKAKQV---IEREgaLKL Saadavllxealdnpavvnaklklase
>MetJ  aeHGKKSEQVKKITVSIPLKVLKLTLDERT---RRKvnnlrhATNSELLCEAFLHAFTGQplpddadlrkersdeipeaakeIMREMG---inpetweyx
>ParG  TAPVSSGKIKRVNWNFDEEKHTRFKAACAR----KG-----TSITDVMNQLVDNWLKENE
>FitA  ASVVIIRLSEATHNAIKFRAR----AA-----GRSTEAIEIRLILDNLAKAQ---Q-TVRLGSMLasigqeiggvel

```

Figure S6



Supplemental Table S0: Molecular Dynamics (anneal.inp) and NCS parameters used for E73 Structure Calculations

Simulated annealing protocol: torsion, torsion, cartesian, minimization

Calculated structures: 100

High temperature torsion dynamics:

temp.	50,000 K
# steps	2000
time/step	60 ps
NOE scale factor	150
VDW scale factor	0.1
Dihedral restraints scale factor	100

1st cooling stage:

temp.	50,000 => 0 K
# steps	2000;
time/step	60 ps
temp. step	250
NOE scale factor	150
VDW scale factor	0.1=>1
Dihedral restraints scale factor	200

2nd cooling stage:

temp.	2000 => 0 K
# steps	15,000
time/step	75 ps
temp. step	25
NOE scale factor	150
VDW scale factor	1->4
Dihedral restraints scale factor	200

Minimization stage:

# steps	2000
NOE scale factor	75
VDW scale factor	1
Dihedral restraints scale factor	400

Non crystallographic symmetry (NCS) Rotation Matrix

NCS operator (which transforms segid A and resid 10:69 and name CA => segid B and resid 10:69 and name CA)

rotation matrix = (0.16066 -0.82741 0.53813)
(-0.86939 -0.37675 -0.31972)
(0.46728 -0.41648 -0.77987)

translation vector (0.05499 0.24328 0.15567)

Table S1 – ^{15}N -Relaxation parameters measured for E73 at pH 5.0 and 312 K.

<u>Residue</u> <u>type</u>	<u>Residue</u> <u>number</u>	$\frac{^{15}\text{N}-\{^1\text{H}\}}{\text{nOe (I/Io)}}$	$\frac{^{15}\text{N}-\{^1\text{H}\}}{\text{err (I/Io)}}$ nOe	$\frac{^{15}\text{N}-T_1}{\text{(ms)}}$	$\frac{^{15}\text{N}-T_1}{\text{error (ms)}}$	$\frac{^{15}\text{N}-T_2}{\text{(ms)}}$	$\frac{^{15}\text{N}-T_2}{\text{err (ms)}}$
MET	1	-	-	-	-	-	-
VAL	2	-0.29	0.01	772.9	7.4	245.7	14.9
GLU	3	-0.28	0.01	758.1	52.5	311.1	3.7
SER	4	-	-	-	-	-	-
LYS	5	-	-	-	-	-	-
LYS	6	-	-	-	-	-	-
ILE	7	0.12	0.01	725.8	6.2	156.4	1.2
ALA	8	0.34	0.01	684.7	4.0	113.7	1.8
LYS	9	0.57	0.03	758.1	33.0	89.9	2.2
LYS	10	0.70	0.01	734.8	0.2	84.9	3.5
LYS	11	-	-	-	-	-	-
THR	12	0.72	0.02	760.8	8.8	74.0	0.7
THR	13	-	-	-	-	-	-
LEU	14	0.70	0.02	725.7	5.7	81.1	0.2
ALA	15	0.67	0.03	721.7	41.5	89.7	1.9
PHE	16	-	-	-	-	-	-
ASP	17	0.78	0.01	783.2	9.4	79.6	5.3
GLU	18	0.76	0.01	705.1	14.5	67.1	0.1
ASP	19	0.74	0.01	735.6	20.6	64.2	1.7
VAL	20	0.74	0.04	759.3	9.9	68.0	1.8
TYR	21	0.79	0.01	767.4	82.4	61.1	2.0
HIS	22	0.80	0.01	675.7	7.6	70.4	1.0
THR	23	0.74	0.02	769.4	91.9	63.6	0.5
LEU	24	-	-	-	-	-	-
LYS	25	0.80	0.01	797.6	6.8	62.2	0.3
LEU	26	0.78	0.01	795.1	2.1	64.3	0.1
VAL	27	0.70	0.03	739.3	10.3	81.8	1.6
SER	28	0.80	0.03	743.3	1.6	62.8	0.1
VAL	29	0.81	0.02	777.6	29.1	62.8	3.1
TYR	30	0.78	0.01	749.3	15.1	67.3	0.1
LEU	31	0.73	0.02	718.9	25.3	66.9	0.1
ASN	32	0.75	0.01	919.2	8.3	64.7	0.3
ARG	33	0.78	0.01	864.2	19.9	61.5	1.4
ASP	34	0.68	0.01	847.1	10.8	74.2	0.8
MET	35	0.71	0.03	728.5	17.0	68.6	3.2
THR	36	0.75	0.01	675.5	11.9	73.6	0.2
GLU	37	0.75	0.06	706.3	13.2	73.8	0.9
ILE	38	-	-	-	-	-	-

<u>Residue</u> <u>type</u>	<u>Residue</u> <u>number</u>	$\frac{^{15}\text{N}-\{^1\text{H}\}}{\text{nOe (I/Io)}}$	$\frac{^{15}\text{N}-\{^1\text{H}\} \text{ nOe}}{\text{error (I/Io)}}$	$\frac{^{15}\text{N}-\text{T}_1}{(\text{ms})}$	$\frac{^{15}\text{N}-\text{T}_1}{\text{error (ms)}}$	$\frac{^{15}\text{N}-\text{T}_2}{(\text{ms})}$	$\frac{^{15}\text{N}-\text{T}_2}{\text{error (ms)}}$
ILE	39	0.83	0.01	690.7	13.9	70.5	2.5
GLU	40	0.80	0.02	683.4	7.8	69.7	0.7
GLU	41	0.81	0.01	702.3	26.8	70.3	1.7
ALA	42	0.79	0.01	683.1	1.8	68.5	0.7
VAL	43	0.75	0.01	760.1	8.4	71.2	0.6
VAL	44	0.77	0.02	716.0	5.2	62.6	0.2
MET	45	0.75	0.02	753.0	15.2	59.6	0.5
TRP	46	0.78	0.01	690.2	89.7	71.2	0.8
LEU	47	0.75	0.03	727.3	1.2	68.5	2.4
ILE	48	0.76	0.03	701.7	20.2	70.0	1.1
GLN	49	0.77	0.01	734.5	15.0	67.2	0.4
ASN	50	0.78	0.01	791.5	11.0	73.9	1.7
LYS	51	0.71	0.02	758.7	6.9	70.5	0.4
GLU	52	0.74	0.01	676.0	8.8	73.8	0.8
LYS	53	0.69	0.01	725.6	7.7	73.8	0.3
LEU	54	0.68	0.01	767.7	8.9	76.6	0.6
PRO	55	-	-	-	-	-	-
ASN	56	0.75	0.03	727.3	1.2	68.5	2.4
GLU	57	-	-	-	-	-	-
LEU	58	0.73	0.01	734.8	7.8	68.9	0.3
LYS	59	0.79	0.01	708.6	17.6	69.9	0.1
PRO	60	-	-	-	-	-	-
LYS	61	0.69	0.02	767.5	0.4	70.3	1.7
ILE	62	0.74	0.01	737.6	93.3	69.9	0.9
ASP	63	-	-	-	-	-	-
GLU	64	0.75	0.01	772.2	13.1	68.9	0.5
ILE	65	0.68	0.05	753.3	7.6	67.1	0.2
SER	66	0.79	0.01	705.9	3.1	68.6	0.4
LYS	67	0.74	0.00	692.2	9.6	70.6	0.9
ARG	68	0.75	0.01	731.4	4.0	69.1	0.6
PHE	69	0.69	0.01	733.8	10.2	72.9	2.1
PHE	70	0.62	0.01	749.9	59.0	87.1	0.4
PRO	71	-	-	-	-	-	-
ALA	72	0.16	0.01	779.6	50.7	177.1	5.0
LYS	73	-0.64	0.01	1003.2	9.7	471.1	1.6

Table S2. Spectral density values for E73 measured at 14.1 T.

<u>Residue type</u>	<u>Residue no.</u>	<u>$J_{\text{eff}}(0)$, ns/rad</u>	<u>$J(\omega_N)$, ns/rad</u>	<u>$J(0.87\omega_H)$, ps/rad</u>
MET	1	-	-	-
VAL	2	1.28 ± 0.10	0.27 ± 0.01	25.96 ± 0.30
GLU	3	0.94 ± 0.02	0.28 ± 0.02	26.35 ± 1.78
SER	4	-	-	-
LYS	5	-	-	-
LYS	6	-	-	-
ILE	7	2.16 ± 0.02	0.31 ± 0.01	19.16 ± 0.26
ALA	8	3.06 ± 0.05	0.34 ± 0.01	15.03 ± 0.46
LYS	9	3.98 ± 0.10	0.32 ± 0.01	8.44 ± 1.09
LYS	10	4.23 ± 0.18	0.33 ± 0.01	6.36 ± 0.01
LYS	11	-	-	-
THR	12	4.90 ± 0.05	0.32 ± 0.01	5.93 ± 0.86
THR	13	-	-	-
LEU	14	4.43 ± 0.01	0.34 ± 0.01	6.89 ± 0.89
ALA	15	3.98 ± 0.10	0.34 ± 0.02	7.59 ± 1.40
PHE	16	-	-	-
ASP	17	4.55 ± 0.32	0.32 ± 0.01	4.59 ± 0.58
GLU	18	5.41 ± 0.01	0.35 ± 0.01	5.32 ± 0.44
ASP	19	5.67 ± 0.16	0.33 ± 0.01	5.52 ± 0.17
VAL	20	5.35 ± 0.15	0.33 ± 0.01	4.74 ± 1.51
TYR	21	5.99 ± 0.19	0.32 ± 0.03	4.26 ± 0.46
HIS	22	5.13 ± 0.08	0.37 ± 0.01	4.62 ± 0.43
THR	23	5.74 ± 0.05	0.32 ± 0.04	4.87 ± 1.09
LEU	24	-	-	-
LYS	25	5.90 ± 0.03	0.31 ± 0.01	3.90 ± 0.19
LEU	26	5.69 ± 0.01	0.31 ± 0.01	4.32 ± 0.40
VAL	27	4.40 ± 0.09	0.33 ± 0.01	5.90 ± 1.22
SER	28	5.81 ± 0.00	0.33 ± 0.01	4.63 ± 1.30
VAL	29	5.83 ± 0.31	0.32 ± 0.01	4.02 ± 0.76
TYR	30	5.41 ± 0.01	0.33 ± 0.01	4.56 ± 0.10
LEU	31	5.43 ± 0.01	0.34 ± 0.01	5.42 ± 0.91
ASN	32	5.68 ± 0.02	0.27 ± 0.01	4.08 ± 0.17
ARG	33	5.98 ± 0.14	0.29 ± 0.01	3.98 ± 0.20
ASP	34	4.91 ± 0.06	0.29 ± 0.01	5.89 ± 0.56
MET	35	5.30 ± 0.25	0.34 ± 0.01	5.77 ± 1.28
THR	36	4.90 ± 0.02	0.36 ± 0.01	6.00 ± 0.12
GLU	37	4.90 ± 0.06	0.35 ± 0.01	4.43 ± 2.63
ILE	38	-	-	-
ILE	39	5.14 ± 0.19	0.36 ± 0.01	4.07 ± 0.42

<u>Residue type</u>	<u>Residue no.</u>	<u>$J_{\text{eff}}(0)$, ns/rad</u>	<u>$J(\omega_N)$, ns/rad</u>	<u>$J(0.87\omega_H)$, ps/rad</u>
GLU	41	5.15 ± 0.14	0.35 ± 0.01	3.99 ± 0.46
ALA	42	5.29 ± 0.06	0.36 ± 0.01	5.01 ± 0.45
VAL	43	5.10 ± 0.05	0.33 ± 0.01	4.94 ± 0.40
VAL	44	5.82 ± 0.02	0.35 ± 0.01	4.80 ± 0.71
MET	45	6.14 ± 0.06	0.33 ± 0.01	4.98 ± 0.83
TRP	46	5.08 ± 0.07	0.36 ± 0.05	4.98 ± 0.64
LEU	47	5.31 ± 0.20	0.34 ± 0.01	4.95 ± 1.48
ILE	48	5.17 ± 0.08	0.35 ± 0.01	4.91 ± 1.34
GLN	49	5.42 ± 0.04	0.34 ± 0.01	4.67 ± 0.45
ASN	50	4.92 ± 0.12	0.31 ± 0.01	4.13 ± 0.40
LYS	51	5.16 ± 0.03	0.32 ± 0.01	5.77 ± 0.63
GLU	52	4.88 ± 0.06	0.36 ± 0.01	6.00 ± 0.26
LYS	53	4.90 ± 0.02	0.34 ± 0.01	6.89 ± 0.05
LEU	54	4.73 ± 0.04	0.32 ± 0.01	6.29 ± 0.43
PRO	55	-	-	-
ASN	56	5.31 ± 0.19	0.34 ± 0.01	4.95 ± 1.52
GLU	57	-	-	-
LEU	58	5.27 ± 0.02	0.33 ± 0.01	5.73 ± 0.23
LYS	59	5.18 ± 0.01	0.35 ± 0.01	4.84 ± 0.67
PRO	60	-	-	-
LYS	61	5.17 ± 0.14	0.32 ± 0.01	5.88 ± 0.97
ILE	62	5.19 ± 0.07	0.33 ± 0.04	5.52 ± 0.70
ASP	63	-	-	-
GLU	64	5.28 ± 0.04	0.32 ± 0.01	4.87 ± 0.39
ILE	65	5.42 ± 0.02	0.33 ± 0.01	6.02 ± 1.85
SER	66	5.29 ± 0.04	0.35 ± 0.01	4.65 ± 0.43
LYS	67	5.12 ± 0.07	0.35 ± 0.01	5.84 ± 0.25
ARG	68	5.25 ± 0.05	0.34 ± 0.01	5.13 ± 0.42
PHE	69	4.97 ± 0.15	0.33 ± 0.01	6.58 ± 0.23
PHE	70	4.12 ± 0.03	0.32 ± 0.02	7.68 ± 0.69
PRO	71	-	-	-
ALA	72	1.89 ± 0.06	0.29 ± 0.02	16.77 ± 1.10
LYS	73	0.59 ± 0.01	0.20 ± 0.01	25.58 ± 0.30

Table S3 – Motional parameters computed for E73 using Model-free analysis.

<u>Residue</u> <u>type</u>	<u>Residue</u> <u>number</u>	<u>Model</u>	<u>S²</u>	<u>S²_{err}</u>	<u>S²_f</u>	<u>S²_{f_err}</u>	<u>S²_s</u>	<u>S²_{s_err}</u>	<u>τ_e (ns)</u>	<u>τ_{e_err} (ns)</u>	<u>R_{ex} (s⁻¹)</u>	<u>R_{ex_err}</u> <u>(s⁻¹)</u>
MET	1	-	-	-	-	-	-	-	-	-	-	-
VAL	2	5	0.22	0.02	0.79	0.01	0.28	0.03	772	20	-	-
GLU	3	5	0.14	0.01	0.76	0.04	0.18	0.02	847	16	-	-
SER	4	-	-	-	-	-	-	-	-	-	-	-
LYS	5	-	-	-	-	-	-	-	-	-	-	-
LYS	6	-	-	-	-	-	-	-	-	-	-	-
ILE	7	5	0.39	0.01	0.84	0.01	0.46	0.01	914	10	-	-
ALA	8	5	0.56	0.01	0.91	0.01	0.61	0.01	1009	33	-	-
LYS	9	5	0.77	0.02	0.91	0.02	0.84	0.03	919	233	-	-
LYS	10	5	0.82	0.04	0.92	0.02	0.89	0.02	1267	225	-	-
LYS	11	-	-	-	-	-	-	-	-	-	-	-
THR	12	1	0.96	0.01	-	-	0.96	0.01	-	-	-	-
THR	13	-	-	-	-	-	-	-	-	-	-	-
LEU	14	5	0.88	0.01	0.96	0.01	0.91	0.01	846	231	-	-
ALA	15	5	0.75	0.02	0.91	0.01	0.83	0.04	1333	872	-	-
PHE	16	-	-	-	-	-	-	-	-	-	-	-
ASP	17	1	0.93	0.01	-	-	0.93	0.01	-	-	-	-
GLU	18	1	1.00	0.01	-	-	1.00	0.01	-	-	-	-
ASP	19	4	0.97	0.02	-	-	0.97	0.02	222	387	1.9	0.5
VAL	20	3	0.93	0.01	-	-	0.93	0.01	-	-	1.9	0.4
TYR	21	4	0.89	0.06	-	-	0.89	0.06	15	532	4.6	0.9
HIS	22	1	1.00	0.01	-	-	1.00	0.01	-	-	-	-
THR	23	1	1.00	0.01	-	-	1.00	0.01	-	-	-	-
LEU	24	-	-	-	-	-	-	-	-	-	-	-
LYS	25	-	-	-	-	-	-	-	-	-	-	-
LEU	26	4	0.89	0.01	-	-	0.89	0.01	19	7	3.4	0.1
VAL	27	1	0.93	0.01	-	-	0.93	0.01	-	-	-	-
SER	28	3	0.92	0.01	-	-	0.92	0.01	-	-	3.8	0.1
VAL	29	3	0.89	0.03	-	-	0.89	0.03	-	-	4.0	0.9
TYR	30	4	0.93	0.02	-	-	0.93	0.02	34	53	2.1	0.3
LEU	31	4	0.95	0.03	-	-	0.95	0.03	87	401	2.2	0.4
ASN	32	4	0.76	0.01	-	-	0.76	0.01	12	2	5.0	0.1
ARG	33	4	0.81	0.02	-	-	0.81	0.02	11	2	5.1	0.4
ASP	34	4	0.79	0.02	-	-	0.79	0.02	33	7	2.8	0.2
MET	35	1	1.00	0.01	-	-	1.00	0.01	-	-	-	-

<u>Residue</u> <u>type</u>	<u>Residue</u> <u>number</u>	<u>Model</u>	<u>S²</u>	<u>S² err</u>	<u>S_f²</u>	<u>S_f² err</u>	<u>S_s²</u>	<u>S_s² err</u>	<u>τ_e (ns)</u>	<u>τ_e err (ns)</u>	<u>R_{ex} (s⁻¹)</u>	<u>R_{ex} err</u> <u>(s⁻¹)</u>
THR	36	4	0.90	0.02	-	-	0.90	0.02	1659	195	0.5	0.2
GLU	37	2	0.94	0.01	-	-	0.94	0.01	1409	481	-	-
ILE	38	-	-	-	-	-	-	-	-	-	-	-
ILE	39	1	1.00	0.01	-	-	1.00	0.01	-	-	-	-
GLU	40	1	1.00	0.01	-	-	1.00	0.01	-	-	-	-
GLU	41	1	1.00	0.01	-	-	1.00	0.01	-	-	-	-
ALA	42	1	1.00	0.01	-	-	1.00	0.00	-	-	-	-
VAL	43	1	0.98	0.01	-	-	0.98	0.01	-	-	-	-
VAL	44	-	-	-	-	-	-	-	-	-	-	-
MET	45	3	0.98	0.02	-	-	0.98	0.02	-	-	2.8	0.3
TRP	46	2	0.98	0.01	-	-	0.98	0.01	500	419	-	-
LEU	47	1	1.00	0.01	-	-	1.00	0.01	-	-	-	-
ILE	48	1	1.00	0.01	-	-	1.00	0.01	-	-	-	-
GLN	49	1	1.00	0.01	-	-	1.00	0.00	-	-	-	-
ASN	50	1	0.93	0.01	-	-	0.93	0.01	-	-	-	-
LYS	51	4	0.94	0.01	-	-	0.94	0.01	113	30	0.7	0.2
GLU	52	4	0.89	0.01	-	-	0.89	0.01	1669	158	0.5	0.2
LYS	53	4	0.94	0.01	-	-	0.94	0.01	473	118	0.2	0.1
LEU	54	4	0.90	0.01	-	-	0.90	0.01	70	14	0.7	0.2
PRO	55	-	-	-	-	-	-	-	-	-	-	-
ASN	56	1	1.00	0.01	-	-	1.00	0.01	-	-	-	-
GLU	57	-	-	-	-	-	-	-	-	-	-	-
LEU	58	4	0.93	0.01	-	-	0.93	0.01	73	11	2.0	0.1
LYS	59	1	1.00	0.01	-	-	-	-	-	-	-	-
PRO	60	-	-	-	-	-	-	-	-	-	-	-
LYS	61	4	0.90	0.01	-	-	0.90	0.01	64	24	1.7	0.4
ILE	62	4	0.96	0.06	-	-	0.96	0.06	546	812	0.6	0.9
ASP	63	-	-	-	-	-	-	-	-	-	-	-
GLU	64	4	0.93	0.02	-	-	0.93	0.02	48	21	1.4	0.2
ILE	65	3	0.98	0.01	-	-	0.98	0.01	-	-	1.0	0.1
SER	66	1	1.00	0.01	-	-	1.00	0.01	-	-	-	-
LYS	67	4	0.92	0.01	-	-	0.92	0.01	1298	194	0.9	0.2
ARG	68	1	1.00	0.01	-	-	1.00	0.01	-	-	-	-
PHE	69	2	0.95	0.01	-	-	0.95	0.01	324	196	-	-
PHE	70	2	0.82	0.01	-	-	0.82	0.01	56	7	-	-
PRO	71	-	-	-	-	-	-	-	-	-	-	-
ALA	72	5	0.33	0.02	0.76	0.03	0.44	0.03	1002	41	-	-
LYS	73	5	0.08	0.01	0.62	0.01	0.14	0.01	696	4	-	-